Voxelwise optimization of hemodynamic lags to improve regional CVR estimates in breath-hold fMRI*

Stefano Moia, Rachael C. Stickland, Apoorva Ayyagari, Maite Termenon, César Caballero-Gaudes, and Molly G. Bright

***Abstract*— Cerebrovascular Reactivity (CVR), the responsiveness of blood vessels to a vasodilatory stimulus, is an important indicator of cerebrovascular health. Assessing CVR with fMRI, we can measure the change in the Blood Oxygen Level Dependent (BOLD) response induced by a change in CO_2 pressure (%BOLD/mmHg). However, there exists a temporal offset between the recorded CO_2 pressure and the local BOLD response, due to both measurement and physiological delays. If this offset is not corrected for, voxel-wise CVR values will not be accurate. In this paper, we propose a framework for mapping hemodynamic lag in breath-hold fMRI data. As breath-hold tasks drive task-correlated head motion artifacts in BOLD fMRI data, our framework for lag estimation fits a model that includes polynomial terms and head motion parameters, as well as a shifted variant of the CO_2 regressor (±9 s in 0.3 s increments), and the hemodynamic lag at each voxel is the shift producing the maximum total model R^2 within physiological constraints. This approach is evaluated in 8 subjects with multi-echo fMRI data, resulting in robust maps of hemodynamic delay that show consistent regional variation across subjects, and improved contrast-to-noise compared to methods where motion regression is ignored or performed earlier in preprocessing.**

***Clinical Relevance*— We map hemodynamic lag using breath-hold fMRI, providing insight into vascular transit times and improving the regional accuracy of cerebrovascular reactivity measurements.**

I. Introduction

Cerebrovascular reactivity (CVR), the responsiveness of blood vessels to a vasodilatory stimulus, is rapidly becoming an important biomarker of cerebrovascular health [1-3]. One non-invasive approach to assessing CVR uses simple breathing tasks (e.g. short breath-holds or deep breaths) to modulate CO_2 in a subject-directed but predictable manner [4]. The blood oxygen level dependent (BOLD) functional MRI response is commonly used to assess the dilatory response induced by hypercapnia. The end-tidal partial pressure of CO_2 ($P_{ET}CO_2$), a non-invasive surrogate of arterial CO_2, is typically convolved with a hemodynamic response function and input into a generalized linear model (GLM) to estimate CVR (%BOLD/mmHg). However, there exists a temporal offset between the $P_{ET}CO_2$ measurement and the local BOLD response due to an inherent delay between CO_2 exhalation inside the scanner and CO_2 recording outside (measurement delay), systemic changes in blood gases which travel with blood to arrive at local brain regions (vascular transit delay), and local arterioles responding to blood gas levels differently (vasodilatory dynamics). To improve estimation of CVR amplitude we need to correct for this temporal offset. This challenge has been addressed in multiple ways in the literature. Simple averaging of breath-hold data was used to map CVR time-to-peak in healthy subjects [4], revealing consistent regional variability in CVR lags. In CO_2 inhalation studies, Transfer Function Analysis has been used to measure the phase of the BOLD response [5], and multi-parametric hemodynamic information including Bolus Arrival Time has been extracted using iterative linear regression [6]. The phase of the BOLD response to a sinusoidal CO_2 paradigm efficiently provides similar information [7]. The algorithm *Rapidtide* uses recursive cross-correlation methods to ascertain lags between voxelwise fMRI data and a reference timeseries [8]; in gas inhalation studies where $P_{ET}CO_2$ acts as the reference, this algorithm successfully maps CVR latency in control and clinical populations, highlighting that hemodynamic lag is a sensitive measure of regional pathology [9]. In resting state data, *Rapidtide* can estimate systemic vascular processes via the global fMRI signal and extract similar hemodynamic lag maps [10]. Yet, the global fMRI signal might also include severe motion-related confounds and irrelevant physiological processes that can degrade the quality of the estimates. An alternative GLM approach to optimize lag during CVR fitting proposed the orthogonalization of the reference $P_{ET}CO_2$ signal to the motion parameters [11]. Although this approach showed reproducible measures of BOLD CVR, the modified $P_{ET}CO_2$ signal can potentially bias CVR amplitudes.

In this paper, we estimate the hemodynamic lag in breath-hold BOLD fMRI data while preserving semi-quantitative measures of CVR amplitude. Breath-hold CVR experiments

*Research supported by the Eunice Kennedy Shriver National Institute of Child Health and Human Development of the National Institutes of Health under award number K12HD073945, the European Union's Horizon 2020 research and innovation program (Marie Skłodowska-Curie grant agreement No. 713673), a fellowship from La Caixa Foundation (ID 100010434, fellowship code LCF/BQ/IN17/11620063), the Spanish Ministry of Economy and Competitiveness (Ramon y Cajal Fellowship, RYC-2017-21845), the Spanish State Research Agency (BCBL "Severo Ochoa" excellence accreditation, SEV- 2015-490), the Basque Government (BERC 2018-2021 and PIBA_2019_104), the Spanish Ministry of Science, Innovation and Universities (MICINN; FJCI-2017-31814). *Stefano Moia and Rachael Stickland are co-first authors.*

S. Moia, M. Termenon, and C. Caballero-Gaudes are with the Basque Center on Cognition Brain and Language, San Sebastián, Spain (e-mail: s.moia@bcbl.eu; m.termenon@bcbl.eu; c.caballero@bcbl.eu).

R C. Stickland, A. Ayyagari, and M. G. Bright are with the Department of Biomedical Engineering and the Department of Physical Therapy and Human Movement Science, Northwestern University, Chicago, IL 60091 USA (e-mail: molly.bright@northwestern.edu; apoorva.ayyagari@northwestern.edu; rachael.stickland@northwestern.edu).

require minimal additional equipment compared to gas inhalation, and may provide more robust lag estimates than resting state data [12], making them an attractive approach for clinical and research settings. However, subjects tend to take deep recovery breaths after the breath-hold, which can lead to severe task-correlated head motion [4]. To address this, we identify the optimal temporal shift between a $P_{ET}CO_2$ model and the BOLD time-series for every voxel, based on maximizing full model fit within physiological constraints. Unlike averaging, cross-correlation or regression techniques currently in the literature, we construct and fit a regression model that includes nuisance polynomial terms and head motion parameters as well as a shifted variant of the $P_{ET}CO_2$ regressor, without orthogonalization. While motion regression is a typical preprocessing step, having sequential steps for denoising and lag estimation, as done in cross-correlation approaches, might lead to biased estimates and/or reintroduction of motion effects [13]. Due to task-correlated motion in breath-hold data, with an unknown temporal offset between local motion-related fMRI artifacts and $P_{ET}CO_2$ recordings, simultaneous fitting more accurately addresses these collinearities [13]. We compare our simultaneous fitting approach to other lag-optimization strategies incorporating motion correction in the literature. Finally, we demonstrate consistent regional variability in hemodynamic lag across subjects, examine the contrast within lag maps, and show how accounting for lag impacts regional CVR estimates.

II. Methods

A. Data Acquisition

Ten neurotypical subjects (5F, aged 25-40y) were scanned on a 3T Siemens PrismaFit MR scanner. In the CVR scan, a multi-echo gradient-echo echo-planar imaging BOLD fMRI scan (ME-fMRI) was acquired (340 volumes, TR = 1.5 s, TEs = 10.6/28.69/46.78/64.87/82.96 ms, FA = 70°, MB = 4, GRAPPA = 2, 52 slices, Partial-Fourier = 6/8, FoV = 211x211 mm², voxel size = 2.4x2.4x3 mm³). High-resolution T2-weighted (T2-w) Turbo Spin Echo and T1-weighted (T1-w) MP2RAGE images (176 slices, FoV read = 256 mm, voxel size = 1x1x1 mm³) were also acquired. The breath-hold paradigm [14] included 8 breath-hold trials (Fig. 1). Expired CO_2 was sampled with a nasal cannula connected to a ML206 ADInstruments gas analyzer and recorded at 100 kHz with a MP150 BIOPAC monitoring system.

B. Data Pre-processing

Analysis of Functional NeuroImages (AFNI, 19.3.5 'Nero') and FMRIB Software Library (FSL, 5.0.9) were used. The T1-w and T2-w images were skull-stripped and co-registered. The T1-w image was segmented with Atropos [15] to create masks of gray matter (GM) and white matter (WM). The T1-w image was normalized to the 2.5mm isotropic MNI152 template while the T2-w volume was co-registered to a skull-stripped EPI single-band reference image (SBRef). Head re-alignment to the SBRef was performed on the first echo and applied to the other volumes with MCFLIRT and FLIRT. Data from five echoes were optimally combined to improve

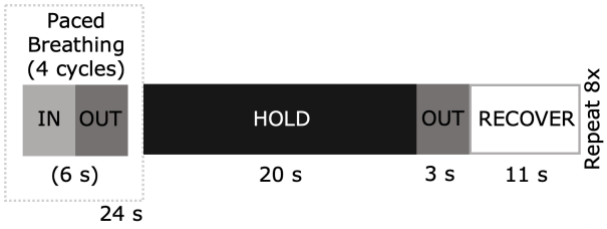

Figure 1. Schematic of the breath-hold paradigm. Participants were cued visually within the scanner. The brief exhalation after the hold is important for obtaining a $P_{ET}CO_2$ estimate of the hypercapnia induced by each hold.

the contrast to noise ratio[16] using tedana[17], and distortion field correction was performed using FSL topup procedure.

C. Lag Optimization and CVR calculation

The end-tidal peaks of the CO_2 trace were automatically identified and manually inspected. The $P_{ET}CO_2$ trace was down-sampled to 40 Hz for ease of handling, demeaned and convolved with the canonical HRF ($P_{ET}CO_2$*hrf*) (Python3). $P_{ET}CO_2$*hrf* was shifted to maximize the cross-correlation with the up-sampled average GM time-course (bulk shift) in order to account for measurement delay and a general vascular transit delay. Then, 60 shifted versions of $P_{ET}CO_2$*hrf* were created, between ±9 s from the bulk shift, with an increment of 0.3 s (fine shift). A range of ±9 s is based on previous literature [e.g. 4, 9, 10, 11, 18], finding few consistent reports of relative lags of ±8 s in healthy subjects. For each shifted $P_{ET}CO_2$*hrf* trace, a generalized linear model (GLM) was constructed including: a shifted $P_{ET}CO_2$*hrf* regressor (down-sampled to TR), 6 realignment parameters and their derivatives (demeaned), and up to 3rd order Legendre polynomials. The resulting GLM design matrices, identical except for fine shifting of $P_{ET}CO_2$*hrf*, were fit to the optimally combined ME-fMRI data (3dDeconvolve). The optimal fine shift at each voxel was identified as maximizing the full model coefficient of determination (R^2) to account for possible collinearities between regressors [19]. Then, these lag maps were clipped at ±8.4 s to remove voxels in which optimization resolved at or adjacent to the boundary, where fit may not be truly optimized and literature suggests lag may not be physiologically plausible. The beta coefficient of the $P_{ET}CO_2$*hrf* regressor at optimum shift was retrieved and scaled by the fitted mean of that voxel timeseries. This created an optimized hemodynamic lag map and a lag-corrected CVR map in %BOLD/mmHg, with associated CVR t-statistics. We termed this lag optimization procedure simultaneous motion fitting (LagOpt-SimMot) and compare it with an un-optimized model only applying the bulk shift to the $P_{ET}CO_2$*hrf* regressor (NoOpt). We also compare it to a GLM with no motion regression (LagOpt-NoMot) and an approach that included only shifted $P_{ET}CO_2$*hrf* regressors in the GLM but regressed out motion parameters and Legendre Polynomials beforehand, i.e. a sequential approach (LagOpt-SeqMot).

D. Group maps and summary statistics

CVR maps, t-statistic maps and lag maps were normalized to the MNI template, then averaged across subjects. Group

average CVR maps do not include voxel data from subjects where lag was deemed implausible, or where the CVR fit was not deemed significant. Un-optimized (bulk shift only) CVR maps were thresholded at $t>1.65$ ($p<0.05$, 313 DoF). To account for multiple comparisons, lag-optimized (bulk and fine shift) CVR maps were thresholded at $t>3.164$, equivalent to $p<0.05$ adjusted with Šidák correction [12] (313 DoF). Four regions of interest (ROIs) were created by segmenting the MNI template into GM and WM (eroded with a 4mm gauss kernel to avoid partial volume effects). A mask of the putamen (Harvard-Oxford Subcortical structural atlas) and a mask of cerebellar GM (Cerebellar MNI atlas) were obtained, and both subtracted from the GM mask. Putamen and cerebellum ROIs were chosen due to their previously reported earlier and later hemodynamic lags, respectively [4]. For each subject, mean values over each ROI were extracted from lag-optimized CVR and un-optimized CVR maps, and paired t-tests were done to assess statistical differences. Similar maps were created for LagOpt-NoMot and LagOpt-SeqMot. The Contrast to Noise Ratios (CNR) of lag values between ROIs, and CVR in each ROI, were compared across NoMot, SeqMot and SimMot, and paired t-tests assessed statistical differences.

III. Results

Two subjects were excluded due to poor task performance, leaving eight subjects for final analysis (4F, age 25-40y). Summary lag and CVR statistics are given in Table 1. WM has a delayed response compared to GM and the putamen and cerebellum demonstrate much earlier and later responses, respectively. Average CVR significantly increases after lag optimization (Table 1, Fig. 2). Thus, fine correction for lag variability improves local CVR estimates that would otherwise be underestimated. Fig. 3A shows CVR and lag maps for an example subject and group averages. Fig. 3B compares lag and optimized CVR maps across the SimMot, SeqMot and NoMot methods, with accompanying CNR estimates in Table 2. Lag CNR increased using the SimMot method, however only GM-Cerebellum contrast reached significance, showing an average 18.8% increase. Average CVR values were lower in SimMot compared to both SeqMot and NoMot for GM and Cerebellum ($t(7) > 3$, $p<0.05$).

IV. Discussion

Hemodynamic lag can be successfully mapped in breath-hold fMRI data. Our approach simultaneously fits for CO_2 CVR effects and head motion to reduce the bias of task-correlated motion artifacts in shift optimization. After lag optimization,

TABLE I. Optimized lag values (averaged over each ROI) and CVR values with and without lag optimization. Values are mean±standard deviation across subjects.

ROI	SimMot Lag (sec)	CVR (%BOLD/mmHg)	
		SimMot	***NonOpt***
WM	0.48 ±0.82	0.16 ±0.03	0.09 ±0.02 [a]
GM	-1.30 ±0.56	0.38 ±0.09	0.24 ±0.06 [a]
Putamen	-2.88 ±1.12	0.28 ±0.07	0.18 ±0.05 [a]
Cerebellum	1.53 ±0.72	0.31 ±0.07	0.19 ±0.04 [a]

a. SimMot - NonOpt: significant t-test, DoF=7, $p<0.0001$, two-tailed.

TABLE II. Lag CNR compared between different lag optimized methods. Values are mean±standard deviation across subjects.

ROI 1-ROI 2	CNR[a]		
	SimMot	***SeqMot***	***NoMot***
GM-WM	0.52 ±0.21	0.46 ±0.26 [b]	0.49 ±0.25 [b]
GM-Putamen	0.47 ±0.22	0.44 ±0.21 [b]	0.44 ±0.21 [b]
GM-Cerebellum	0.82 ±0.15	0.69 ±0.17 [c]	0.69 ±0.16 [c]

a. $CNR = |Mean_{ROI1} - Mean_{ROI2}| / Stdev_{AllROIs}$

b. SimMot-SeqMot or SimMot-NoMot: non-significant t-test, DoF=7, $p>0.05$, two-tailed.

c. SimMot-SeqMot or SimMot-NoMot: significant t-test, DoF=7, $p<0.05$, two-tailed.

a CVR increase was seen in all ROIs, demonstrating this is an important step to ensure accurate regional CVR values. Lag maps were spatially consistent with previous findings using alternative algorithms and hypercapnic stimuli [4, 18]. The different lag optimization methods (simultaneous, sequential and no motion regression) showed subtle variation. However, lag CNR was always higher using our simultaneous fitting approach, most notably in the cerebellum, a region that is particularly prone to motion artefacts. We also conjecture that NoMot and SeqMot found higher CVR due to task-correlated motion effects that are not properly handled by these models. We demonstrate that accurate measurement of CVR in a subcortical region using transient $P_{ET}CO_2$ manipulations must account for the vasodilatory lag being different from cortical GM. One quarter of all first ischemic infarcts are subcortical, and measuring CVR in these regions may be particularly important [3]. In line with the literature, we searched for an optimal lag between ±9 s relative to the bulk shift. This range should be adjusted in clinical or healthy aging studies to adequately characterize expected pathological transits [9], but the maximum shift should not be longer than half a breath-hold period, as this may lead to spurious negative correlations between $P_{ET}CO_2$*hrf* and fMRI. Negative CVR values were not considered here, however, the latency of these effects can facilitate the discrimination of neurovascular versus purely vascular signals in fMRI data [20], and these phenomena will be explored in future work. Necessary future work will assess feasibility and utility of these methods in clinical populations.

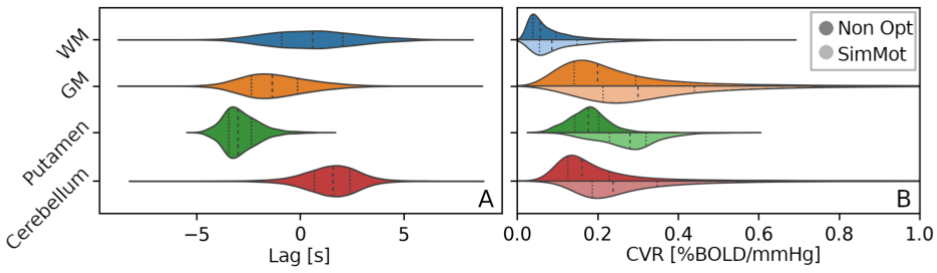

Figure 2. (A) Distribution of group mean lag values in each ROI. WM response is later than GM. Relative to the rest of the GM, the response in the putamen is earlier and the response in the cerebellar GM is much later. (B) Distribution of group mean CVR values with (light colors) and without (dark colors) incorporating the optimal lag.

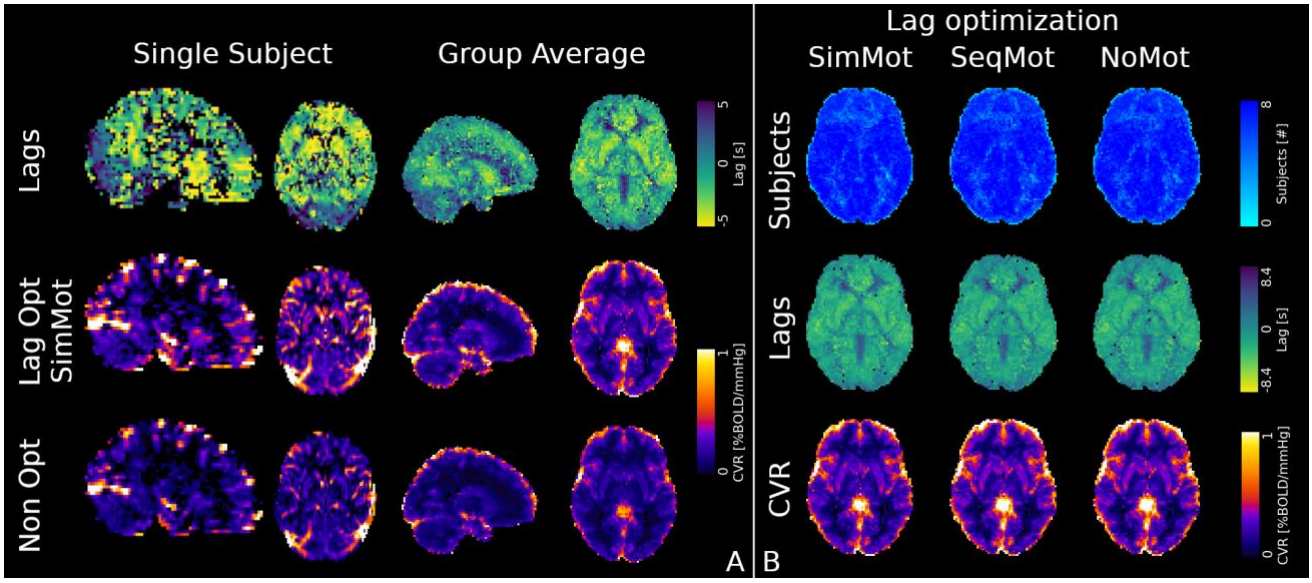

Figure 3. (A) Maps of hemodynamic lag (clipped at ±8.4 s) and CVR, before and after optimization of the temporal shift with the proposed approach (SimMot), for a representative subject and group average. Note the increased contrast between WM and GM after optimal shift, indicating an underestimation of CVR in most brain regions. (B) Group average maps of hemodynamic lag (second row) and CVR (third row) after optimal shift for simultaneous motion regression (SimMot), sequential motion regression (SeqMot) and no motion regression (NoMot). The maps of the first row depict the number of subjects contributing to each voxelwise estimate of lag and CVR after boundary conditions are considered, showing more subjects consistently at the boundary condition at the edges of the brain and WM. SimMot results in improved regional contrast in the lag maps as quantified in Table 2.

REFERENCES

[1] J.J. Pillai and D.J. Mikulis, "Cerebrovascular Reactivity Mapping: An Evolving Standard for Clinical Functional Imaging," *American Journal of Neuroradiology*, vol. 36, no. 1, pp.7-13, Jan. 2015.

[2] A.L. Urback, B. J. MacIntosh and B. I. Goldstein, "Cerebrovascular reactivity measured by functional magnetic resonance imaging during breath-hold challenge: A systematic review," *Neuroscience & Biobehavioral Reviews*, vol. 79, pp. 27-47, Aug. 2017

[3] N. S. Hartkamp, R. P. H. Bokkers, M. J. P. van Osch, G. J. de Borst, and J. Hendrikse, "Cerebrovascular reactivity in the caudate nucleus, lentiform nucleus and thalamus in patients with carotid artery disease," *Journal of Neuroradiology*, vol. 44, no. 2, pp. 143–150, Mar. 2017.

[4] M. G. Bright, D. P. Bulte, P. Jezzard, and J. H. Duyn, "Characterization of regional heterogeneity in cerebrovascular reactivity dynamics using novel hypocapnia task and BOLD fMRI.," *Neuroimage*, vol. 48, no. 1, pp. 166–175, Oct. 2009.

[5] J. Duffin, O. Sobczyk, A. P. Crawley, J. Poublanc, D. J. Mikulis, and J. A. Fisher, "The dynamics of cerebrovascular reactivity shown with transfer function analysis.," *Neuroimage*, vol. 114, pp. 207–216, Jul. 2015.

[6] P. Liu, B. G. Welch, Y. Li, H. Gu, D. King, Y. Yang, M. Pinho, and H. Lu, "Multiparametric imaging of brain hemodynamics and function using gas-inhalation MRI.," *Neuroimage*, vol. 146, pp. 715–723, Feb. 2017.

[7] N. P. Blockley, J. W. Harkin, and D. P. Bulte, "Rapid cerebrovascular reactivity mapping: Enabling vascular reactivity information to be routinely acquired.," *Neuroimage*, vol. 159, pp. 214–223, Jul. 2017.

[8] B. Frederick, T. Salo, and D. M. Drucker, "bbfrederick/rapidtide: January 6, 2020 checkpoint release (Version v1.9.0)", *Zenodo*, http://doi.org/10.5281/zenodo.3598720 , Jan. 6 2020

[9] M. J. Donahue, M. K. Strother, K. P. Lindsey, L. M. Hocke, Y. Tong, and B. D. Frederick, "Time delay processing of hypercapnic fMRI allows quantitative parameterization of cerebrovascular reactivity and blood flow delays.," *J Cereb Blood Flow Metab*, vol. 36, no. 10, pp. 1767–1779, Oct. 2016.

[10] Y. Tong and B. D. Frederick, "Tracking cerebral blood flow in BOLD fMRI using recursively generated regressors.," *Hum. Brain Mapp.*, vol. 35, no. 11, pp. 5471–5485, Nov. 2014.

[11] I. Sousa, P.Vilela, P.Figueiredo, "Reproducibility of hypocapnic cerebrovascular reactivity measurements using BOLD fMRI in combination with a paced deep breathing task," *NeuroImage,* vol. 98, pp. 31-41, Apr. 2014

[12] M. G. Bright, C. R. Tench, and K. Murphy, "Potential pitfalls when denoising resting state fMRI data using nuisance regression.," vol. 154, pp. 1–10, Dec. 2016.

[13] M. A. Lindquist, S. Geuter, T. D. Wager, and B. S. Caffo, "Modular preprocessing pipelines can reintroduce artifacts into fMRI data.," *Hum. Brain Mapp.*, vol. 40, no. 8, pp. 2358–2376, Jun. 2019.

[14] M. G. Bright and K. Murphy, "Reliable quantification of BOLD fMRI cerebrovascular reactivity despite poor breath-hold performance.," *Neuroimage*, vol. 83, pp. 559–568, Dec. 2013.

[15] B. B. Avants, N. J. Tustison, J. Wu, P. A. Cook, and J. C. Gee, "An open source multivariate framework for n-tissue segmentation with evaluation on public data.," *Neuroinformatics*, vol. 9, no. 4, pp. 381–400, Dec. 2011.

[16] S. Posse, S. Wiese, D. Gembris, K. Mathiak, C. Kessler, M. L. Grosse-Ruyken, B. Elghahwagi, T. Richards, S. R. Dager, and V. G. Kiselev, "Enhancement of BOLD-contrast sensitivity by single-shot multi-echo functional MR imaging.," *Magn. Reson. Med.*, vol. 42, no. 1, pp. 87–97, Jul. 1999.

[17] E. DuPre, T. Salo, R. Markello, P. Kundu, K. Whitaker, and D. Handwerker, "ME-ICA/tedana: 0.0.6 (Version 0.0.6)", *Zenodo*, http://doi.org/10.5281/zenodo.2558498 , Feb. 6, 2019.

[18] N. P. Blockley, I. D. Driver, S. T. Francis, P. A. Gowland, "An improved method for acquiring cerebrovascular reactivity maps," *MRM*, vol. 65, no. 5, pp. 1278-1286, May 2011.

[19] J. A. Mumford, J. B. Poline, and R. A. Poldrack, "Orthogonalization of regressors in fMRI models." *PloS one*, vol. 10, no. 4, April 2015.

[20] M. G. Bright, M. Bianciardi, J. A. de Zwart, K. Murphy, and J. H. Duyn, "Early anti-correlated BOLD signal changes of physiologic origin.," *NeuroImage*, vol. 87, pp. 287–296, Nov. 2013.